

Structural Changes in the Skeletal Muscle Fiber of Adult Male Albino Rat Following Atorvastatin Treatment; the Possible Mechanisms of Atorvastatin Induced Myotoxicity

Sahar Ahmed Mokhmer¹, Entesar Ali Saber², Azza Hussien Hamouda¹ and Rehab Ahmed Rifaai^{1*}

¹Department of Histology and cell biology, Faculty of Medicine, Minia University, Egypt

²Faculty of Medicine, Department of Histology and cell biology, Minia University, delegated to Deraya University. New Minia

Abstract

Background: Statins are the most effective and best tolerated agents for treating hyperlipidemia. They have many side effects. The most common side effect in statins users is myopathy.

Aim: This study is concerned with the description of structural changes in rat skeletal muscle following administration of different doses of atorvastatin and identification of the different mechanisms involved in these changes.

Method: Rats were divided randomly into four groups; each group included 6 rats: Group I, the control group, received distilled water. Group II received 10 mg/kg/day of atorvastatin. Group III received 40 mg/kg/day of atorvastatin. Group IV received 80 mg/kg/day of atorvastatin. Atorvastatin was given for 8 weeks. Vastus medialis muscle was taken out, rapidly fixed and processed for histological, histochemical and immunohistochemical studies.

Results: Atorvastatin administration caused morphological changes in the skeletal muscle fibers and in the nerve fibers. Degeneration was more obvious in high doses treated groups. Gleys stain showed nerve degeneration. Succinate dehydrogenase (SDH) staining revealed that SDH activity was affected in type II skeletal muscle fibers and with increasing the dose SDH activity in type I muscle fibers also affected. Moreover acetylcholine esterase (AChE) activity became affected with the doses of 40, 80 mg/kg of atorvastatin. Immunohistochemical studies using myosin heavy chain antibodies revealed degeneration of the type II fibers. However, affection of the type I fibers was observed in 80 mg/kg treated group. Morphometric studies showed an increase in the percent of caspase 3-immuno positive muscle fiber in all treated group.

Conclusion: Atorvastatin has atoxic effect on the skeletal muscle and its nerve supply and this effect is dose dependent. Type II muscle fibers were involved with low dose while type I fibers affected with high dose. Mitochondrial damage, apoptosis of the muscle fiber and decreased AChE activity could be the mechanisms through which atorvastatin induces its toxic effect.

Keywords: Atorvastatin; Myotoxicity rat

Introduction

Statins are drugs used in the treatment of many diseases including hypercholesterolemia, ischemic heart disease (angina, chronic heart disease and myocardial infarction), cerebrovascular accidents and peripheral arterial disease. Adults with a history of cardiovascular disease (CVD) or those with a 10-year risk of developing CVD should start statin therapy as a prophylactic measure. As a result of all these indications, statins are one of the world's most prescribed drugs [1]. Many forms of statins are present in the markets including atorvastatin (Lipitor), lovastatin (Mevacor, Altacor) and simvastatin (Zocor). Inhibition of 3-hydroxy-3-methyl glutaryl coenzyme A reductase (HMG-CoA reductase), a key enzyme in the cholesterol biosynthetic pathway is the mode of action of most of the statins [2].

Many side-effects must be understood and prevented throughout the use of statins. The most severe side-effect is rhabdomyolysis, which is characterized by damaging of the skeletal muscle which leads to the release of muscle proteins into the blood [3]. Statin induces rhabdomyolysis that can be acute, subacute, or chronic, and may be permanent despite dose reduction or substitutions [4].

Myoglobin release from the damaged muscle can lead to acute renal failure. All statins have been associated with adverse muscle events [5]. Statins lower the concentration of low-density lipoprotein

cholesterol and very-low-density lipoprotein cholesterol in people with elevated triglycerides. Many patients cannot reach this at low doses, so they tend to use high doses of statin. The risk of myopathy is increased with high doses [3]. The mechanism determining muscle damage is not clear [6]. There are several possible mechanisms such as depletion of secondary metabolic intermediates and induction of apoptosis, have been proposed for statin-induced myopathy [7]. In the markets atorvastatin is available in 10, 20, 40, and 80 mg tablets. The aim of the present study was to test the effect of different doses of atorvastatin on the skeletal muscles of male albino rat and the possible mechanisms involved in this effect by using histological, histochemical and immunohistochemical methods.

***Corresponding author:** Rehab Ahmed Rifaai, Faculty of Medicine, Department of Histology and cell biology, Minia University, Egypt, Tel: 01003358376; E-mail: rehabrifaai@yahoo.com

Received November 14, 2016; **Accepted** January 10, 2017; **Published** January 15, 2017

Citation: Ahmed S, Saber EA, Hamouda AH, Rifaai RA (2017) Structural Changes in the Skeletal Muscle Fiber of Adult Male Albino Rat Following Atorvastatin Treatment; the Possible Mechanisms of Atorvastatin Induced Myotoxicity. J Cytol Histol 8: 442. doi: [10.4172/2157-7099.1000442](https://doi.org/10.4172/2157-7099.1000442)

Copyright: © 2017 Ahmed S, et al. This is an open-access article distributed under the terms of the Creative Commons Attribution License, which permits unrestricted use, distribution, and reproduction in any medium, provided the original author and source are credited.

Material and Methods

Animals

This study was conducted in the Histology department of faculty of Medicine of El-Minia University. The study was dealing with the skeletal muscle tissues of adult male albino rats. Twenty four male albino rats at the age 6-8 weeks, weighting 150-200 grams, specific pathogens free were used. Animals were housed in a clean plastic cage in an air conditioned room under a 12 h light dark cycle.

All animals became acclimatized for at least 7 days before the outset of the study and were given food and water ad-libitum and were kept at constant humidity and temperature. The experiment was approved by the ethical committee for animal handling for research work in Minia University.

Reagents

Atorvastatin (Lipitor[®]) 40 mg tablets (Egyptian International Pharmaceutical Industries Company (EIPICO), company of pharmacy, Egypt) were obtained from the market. The tablets were ground and then the different doses 10, 40 and 80 mg/kg were calculated. Each dose was freshly dissolved in distilled water before the oral intake.

Experimental design

Animals were randomly divided into four groups (six rats each), the control group author included 6 rats were received distilled water and the treated groups received atorvastatin dissolved in distilled water by a gastric tube at different doses for 8 weeks. Group II received 10 mg/kg/day of atorvastatin [8]. Group III received 40 mg/kg/day of atorvastatin [1]. Group IV received 80 mg/kg/day of atorvastatin. Rats from all groups were sacrificed after 8 weeks by decapitation under light halothane anesthesia. Skeletal muscle tissue samples were obtained for tissue preparation. The vastus medialis muscle of the right limb was obtained and divided into two parts. One part was fixed in 10% formal saline for paraffin sections which were stained with hematoxylin and eosin, Glees method (for axons of nerve fibers) and immunohistochemical reagents. The other part was rapidly put in the cryostat for Succinic dehydrogenase and Acetyl choline esterase histochemical study. All the histological and the histochemical Bancroft and Garblo 2008 [9]. Immunohistochemical staining was performed using polyclonal rabbit antibodies (anti-cleaved caspase 3) which was obtained from sigma aldrich and monoclonal mouse antibodies (anti-myosin fast twitch (type II) heavy-chain myosin) which was obtained from thermo scientific. Immunohistochemistry for both was performed on paraffin sections [10]. Sections were deparaffinized, hydrated then washed in 0.1 M phosphate buffer saline (PBS). Endogenous peroxidases were blocked by treatment with H₂O₂ in methanol. non-specific background staining were inhibited through incubation at room temperature for 30 min in 0.3% bovine serum albumin. The sections were incubated with the diluted primary antibodies for cleaved caspase 3 (1:500) and anti-myosin fast twitch (type II) heavy-chain myosin (1:500) for 60 minutes at room temperature. Sections then were washed 3 times each for 5 minutes in buffer and incubated for further 30 minutes with biotinylated secondary antibodies diluted 1:1000, followed by washing. Following further 30 minutes incubation with Vectastain ABC kits (Avidin, Biotinylated horse radish peroxidase Complex) and washing for 10 minutes, the substrate, diaminobenzidine tetra hydrochloride (DAB) in distilled water was added for 5-10 min. The slides were lightly counterstained by hematoxylin. For anti-cleaved caspase 3 positive control human tonsil slides were stained. The positive immunoreactivity

for anti-myosin fast twitch (type II) heavy-chain myosin appeared as brown stained cytoplasm of the immunoreactive cells. The positive immunoreactivity for anti-cleaved caspase 3 appeared as brown cytoplasmic or nuclear staining. Negative control slides were prepared by the same steps except they were incubated with the antibody diluent instead of primary antibody.

Photography

Slides were photographed using Olympus digital camera. Images were saved as jpg and processed using Adobe Photoshop 7 to standardize brightness, contrast and background color.

Morphometric analysis

The procedures utilized a hardware consisting of a high-resolution color digital camera mounted on an Olympus BX51 microscope and connected to a computer.

Quantitative data were collected for 2 parameters:-

The number of degenerated muscle fibers will be counted and graded for fiber quantification, the total number of muscle fibers and the number of degenerated fibers were counted in 10 different adjacent non overlapped fields for the same slide. Three different sections of the same animal were used. They were counted in the 40 high power fields. Degenerated fibers were graded subjectively; mild- up to approximately 20% of fibers affected; moderate-up to 50% of fibers affected and severe-more than 50% of fibers affected [11].

The percentage of caspase-3 positive fibers control tonsil slides were stained was determined in 10 different adjacent non overlapped fields the number of caspase-3 positive was divided by the total number of fibers at the same fields. Three different sections of the same animal were used.

Results

Morphological study

Examination of H and E stained longitudinal sections (LS) of the muscle tissue of the control group revealed that the muscle fibers were long, non-branching, striated and cylinder with acidophilic sarcoplasm. Their nuclei were multiple, elongated, vesicular and peripherally located just beneath the sarcolemma. Some satellite cells were noticed on the surface of the myofibers and fibroblast like cells appeared within the endomysium (Figure 1A). In transverse section

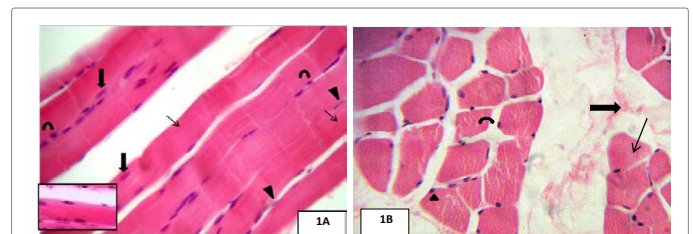


Figure 1: A Photomicrograph of rat skeletal muscle tissue of the control group showing **A.** Bundles of non branching cylindrical shaped muscle fibers with acidophilic sarcoplasm (thin arrows), and multiple elongated vesicular nuclei peripherally located beneath the sarcolemma (thick arrows). Notice the smaller nuclei of satellite cells (curved arrows) and the flat nuclei of fibroblasts in the endomysium (arrow heads). x 400. Inset showing cross striations . X1000. **B.** TS of rat skeletal muscle tissue of the control group showing polygonal shaped skeletal muscle fibers with acidophilic cytoplasm (arrow) and peripherally located nuclei (arrow head). The muscle fibers are separated by endomysium (curved arrow). Notice the perimysium is seen between muscle bundles (thick arrow). (H&E X 400).

(TS), the skeletal muscle fibers appeared polygonal with acidophilic sarcoplasm and peripherally located nuclei. The muscle fibers are grouped into bundles. Each bundle is surrounded by a connective tissue sheath (perimysium). Each muscle fiber is surrounded by endomysium (Figure 1B). In Group II (10 mg/kg atorvastatin treated group), the muscle fibers were more or less with their normal size and longitudinal arrangement. Inflammatory cellular infiltration started through the endomysium (Figure 2A). Some muscle fibers became rounded with loss of the polygonal appearance. Their nuclei appeared rounded central instead of their peripheral position. Splitting of few muscle fibers and fragmentation of the sarcoplasm were observed in both LS and TS (Figures 2A and 2B).

Examination of sections from group III (40 mg/kg atorvastatin treated group), revealed that the LS of the muscle fibrils showed mild wavy appearance. Some myofibers had prominent euchromatic nuclei that were linearly arranged and often surrounded by more satellite cells. Myonuclear changes were also observed in many fibers. These changes were in the form of nuclear enlargement, irregular shapes and clumping. Internal nuclei were also common (Figures 3A and 3B). Inflammatory cellular infiltration was also noticed (Fig.3A) There was

variation in the fiber size. Few muscle fibers appeared hypertrophied with ill defined outlines but most of the fibers still keep their normal appearance. Some of the enlarged fibers appeared splitted and others showed fragmentation of their cytoplasm (Figure 3C).

Regarding sections from group IV (80 mg/kg atorvastatin treated group), the muscle fibers showed disarray of orientation. Their myofibrils became extensively wavy (Figure 4A) Inflammatory cellular infiltration was also noticed in-between the myofibers (Figures 4B and 4C). There was marked variation in the fiber size and most of the myofibers lost their polygonal appearance and appeared swollen. This obscured the endomysium between the deformed myofibers (Figures 4B and 4C). The degenerated muscle fibers appear swollen with pale stained sarcoplasm that was extensively fragmented (Figures 4A and 4C). Some myofibers had prominent euchromatic nuclei that were linearly arranged and often surrounded by more satellite cells (Figure 4D). In the Glee's stained sections of the control group, the nerve fibers showed a continuous uniform impregnation of the silver stain while the myoneural junctions appeared as a hen leg appearance (Figure 5A). In Group II, There was considerable damage of the nerve fibers. This appeared in the form of the breakup of the silver impregnation in comparison with the uniform staining of the control group. Thinning of the nerve fibers was noticed in some areas along their length (Figure 5B). More damage was noticed in group III (Figures 5C and 5D) and IV (Figures 5E and 5F). The degenerated nerve fibers became markedly thin and appeared as ghosts. Silver droplets appeared around the degenerated nerve fiber. Many nerve fibers showed disorganized neurofibrils with breakup of the silver impregnation of this degenerated nerve. Histochemical studies for detection of succinic dehydrogenase enzyme (SDH) activity showed that the transverse section (TS) of the muscular tissue of the control group was consisting mostly of lightly stained (type II) with few deeply stained (type I), the type II fibers are large while type I fibers are small. The staining is granular throughout the fibers (Figure 6A). In group II, some of the low oxidative fast twitch fibers (type II) had central and eccentric loss of staining, while the high oxidative slow twitch fibers (type I) were not affected (Figure 6B). In

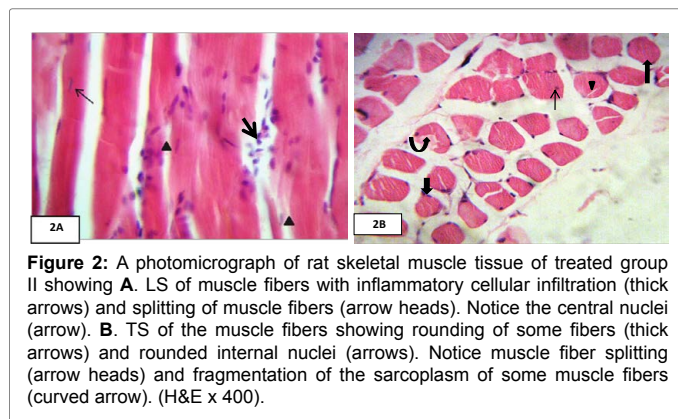


Figure 2: A photomicrograph of rat skeletal muscle tissue of treated group II showing **A.** LS of muscle fibers with inflammatory cellular infiltration (thick arrows) and splitting of muscle fibers (arrow heads). Notice the central nuclei (arrow). **B.** TS of the muscle fibers showing rounding of some fibers (thick arrows) and rounded internal nuclei (arrows). Notice muscle fiber splitting (arrow heads) and fragmentation of the sarcoplasm of some muscle fibers (curved arrow). (H&E x 400).

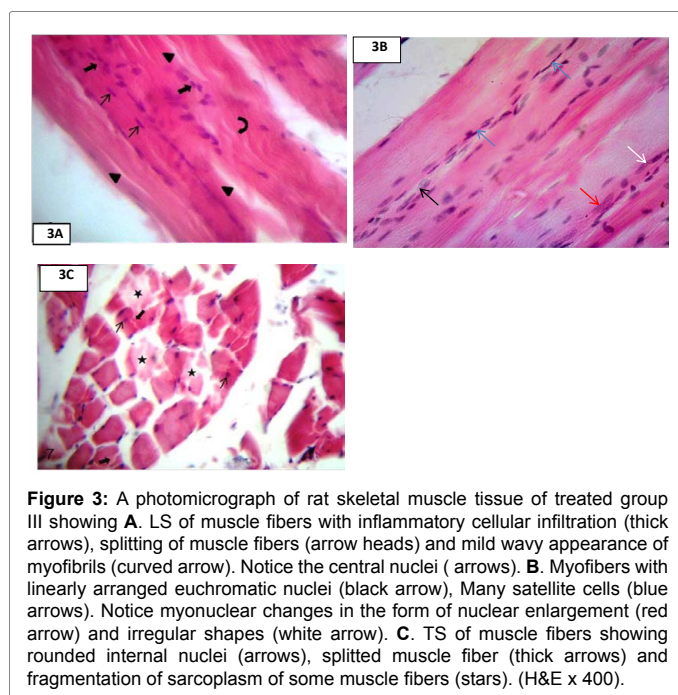


Figure 3: A photomicrograph of rat skeletal muscle tissue of treated group III showing **A.** LS of muscle fibers with inflammatory cellular infiltration (thick arrows), splitting of muscle fibers (arrow heads) and mild wavy appearance of myofibrils (curved arrow). Notice the central nuclei (arrows). **B.** Myofibers with linearly arranged euchromatic nuclei (black arrow), Many satellite cells (blue arrows). Notice myonuclear changes in the form of nuclear enlargement (red arrow) and irregular shapes (white arrow). **C.** TS of muscle fibers showing rounded internal nuclei (arrows), splitted muscle fiber (thick arrows) and fragmentation of sarcoplasm of some muscle fibers (stars). (H&E x 400).

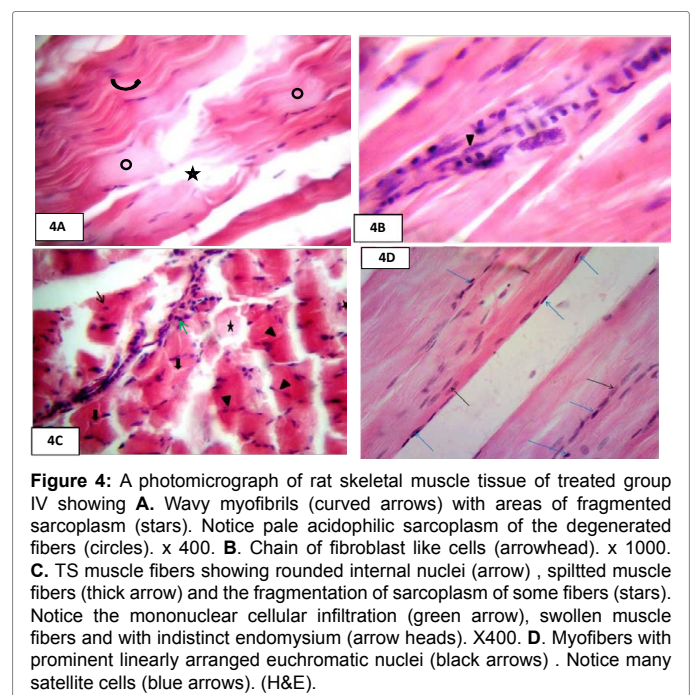


Figure 4: A photomicrograph of rat skeletal muscle tissue of treated group IV showing **A.** Wavy myofibrils (curved arrows) with areas of fragmented sarcoplasm (stars). Notice pale acidophilic sarcoplasm of the degenerated fibers (circles). x 400. **B.** Chain of fibroblast like cells (arrowhead). x 1000. **C.** TS muscle fibers showing rounded internal nuclei (arrow), splitted muscle fibers (thick arrow) and the fragmentation of sarcoplasm of some fibers (stars). Notice the mononuclear cellular infiltration (green arrow), swollen muscle fibers and with indistinct endomysium (arrow heads). X400. **D.** Myofibers with prominent linearly arranged euchromatic nuclei (black arrows). Notice many satellite cells (blue arrows). (H&E).

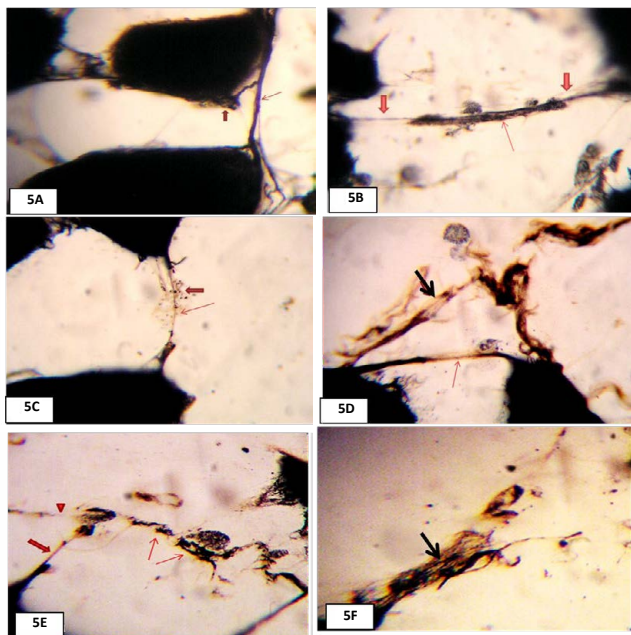


Figure 5: Glee's staining of the skeletal muscle tissue of **A.** Control group showing intact nerve fiber with uniform diameter (arrow). Notice the myoneural junctions (thick arrow) has a hen leg appearance. **B.** Group II showing break up of the nerve fiber staining (arrows) and thinning of some areas along the nerve fiber (thick arrows). **C** and **D.** Group III showing thinning of the nerve fiber (arrow). Notice the droplets of degenerated axon (thick arrow). Notice disorganized neurofibrils (black arrow) of the nerve fiber. **E** and **F.** Group IV showing break up of the nerve fiber staining (arrows) with thinning of the nerve fiber (thick arrow). Some nerve fiber appears as a ghost (arrow head). Others have disorganized neurofibrils (black arrow). (Glee's x 1000).

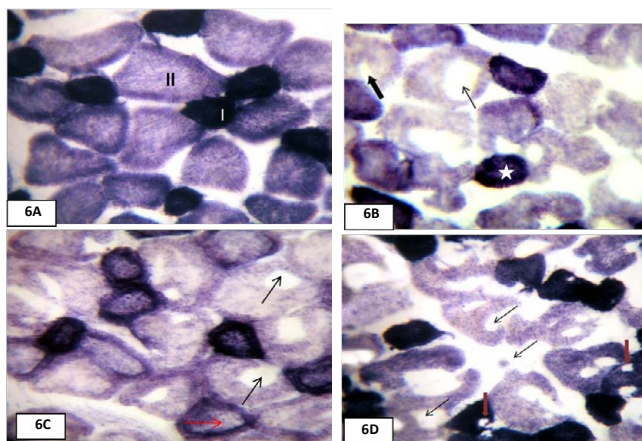


Figure 6: Succinic dehydrogenase histochemical staining of the vastus medialis muscle tissue of **A.** control group showing the muscle consisting mostly of type II fibers with less intensity and few type I fibers with high intensity of staining. **B.** Group II showing type II fibers with central (arrows) and eccentric (thick arrow) loss of staining. Notice sparing of type I fibers (star). **C.** Group III showing central and eccentric loss of staining of type II fibers (arrows). Notice decrease the intensity of staining in the center of type I fibers (red arrow). **D.** Group IV showing complete loss of staining in large areas of type II fibers (arrows). Notice that type I fibers showing eccentric loss of staining (red arrows). (Succinic dehydrogenase histochemistry x 400).

group III, both two types of the muscle fibers were affected. Many low oxidative fast twitch fibers (type II) showed central and eccentric loss of staining. The high oxidative slow twitch fibers (type I) showed decrease

in the intensity of staining in the center (Figure 6C). In group IV the low oxidative fast twitch fibers (type II) had large areas of complete loss of staining, while the highly oxidative slow twitch fibers (type I) showed eccentric loss of staining (Figure 6D). AChE was detected at the motor end plate regions in the different groups. In both the control group (Figure 7A) and group II (Figure 7B), AChE staining showed that the neuromuscular junctions (NMJ) were brown, oval, round or elliptical and compact. They were distributed along the border of the muscle fibers. In group III, some NMJ areas were lightly stained and less compacted when compared to the control group (Figure 7C). NMJ appeared smaller in size, less compacted and lighter in staining in group IV when compared with the previous groups (Figure 7D). Immunohistochemical study of muscle tissues using myosin fast twitch (type II) heavy chain antibody showed that skeletal muscle tissue from the control group had a positive reaction in the form of fine brown granules, the two types of muscle fibers could be demonstrated the more numerous immunopositive type II fast twitch fibers and the less numerous slow twitch muscle fibers (type I) that remained unstained (Figure 8A). For the negative control, slides were prepared from skeletal muscle tissue (Figure 8B). In group II, splitting of some of the immunopositive type II fibers with sparing of the negative immunoreactive type I fibers was noticed (Figure 8C). In group III many type II fibers appeared degenerated with fragmented cytoplasm while the type I fibers retained their normal histological appearance (Figure 8D). Both immunopositive and immunonegative fibers were affected in group IV. Extensive fragmentation of the sarcoplasm appeared in the immunopositive (type II) fibers while some immunonegative (type I) fibers showed splitting (Figure 8E). The positive immunoreactivity for activated caspase 3 appeared in the form of brown coloration of the cytoplasm and/or nuclei of the immunoreactive cells. Positive control slides prepared from human tonsil demonstrated the positive reaction of caspase 3 in the form of fine brown granules (Figure 9A). For the negative control, slides were prepared from skeletal muscle tissue (Figure 9B). Sections of the control group I showed no detectable immunolabeling for activated caspase 3 in the skeletal muscle sections (Figure 10A). In group II, there was obvious high immunoreactivity for activated caspase 3 in the cytoplasm of the rounded muscle fibers. Some immunopositive muscle fibers showed splitting and some nuclei were positively stained (Figure 10B). In group III (Figure 10C) and

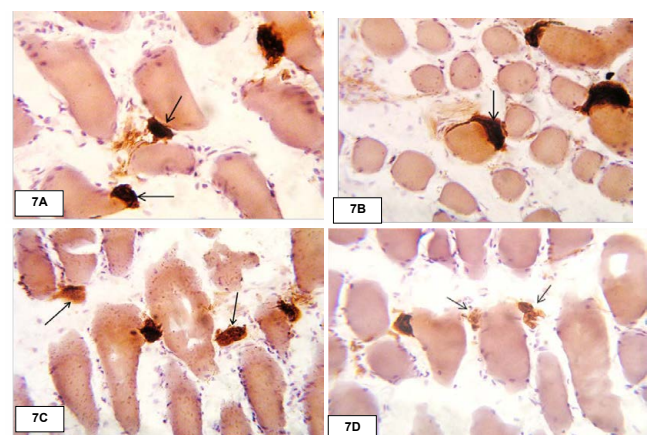


Figure 7: AChE histochemical staining of skeletal muscle tissue of **A.** control group showing brown, oval, round and compact NMJ (neuromuscular junction) areas (arrows) distributed along the border of the muscle fibers. **B.** Group II showing NMJ areas resemble the control group (arrow). **C.** Group III showing some areas of the NMJ are lightly stained (arrows). **D.** Group IV showing small sized lightly stained NMJ areas (arrows). (AChE histochemistry x 400).

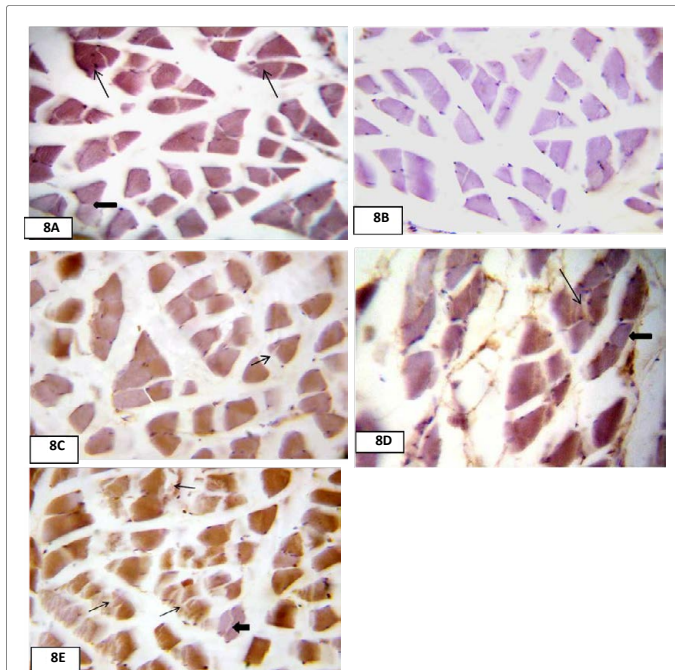


Figure 8: Myosin heavy chain immunohistochemical staining of the vastus medialis muscle tissue of **A.** Positive control group showing positive immunoreactivity in type II fibers (thin arrows) and negative immunoreactivity in type I fibers (thick arrows). **B.** Negative control. **C.** Group II showing splitting of some positive immunoreactive (type II) fibers (arrow). **D.** Group III showing fragmentation of sarcoplasm of immunopositive (type II) fibers (thin arrow) with sparing of immunonegative (type I) fibers (thick arrow). **E.** Group IV showing extensive fragmentation of sarcoplasm of the immunopositive (type II) fibers (thin arrows) and splitting of immunonegative (type I) fibers (thick arrow). (immunohistochemistry counter stain H x 400).

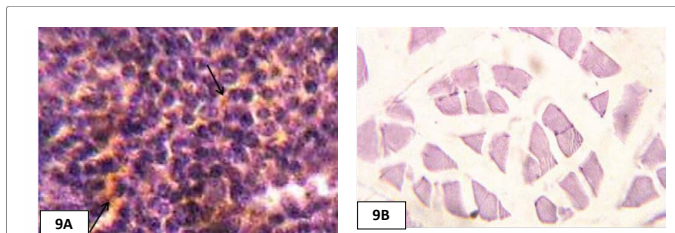


Figure 9: **A.** Positive control tonsillar tissue showing positive immune reaction of caspase 3 (arrows). **B.** Rat skeletal muscle tissue showing a negative reaction in a negative control slide for caspase 3. (immunohistochemistry counter stain H x 400).

group IV (Figure 10D), most of the muscle fibers showed positive cytoplasmic and nuclear expression. Few muscle fibers showed negative immunoreactivity.

The morphometric results

It was found that the percent of fiber degeneration in control rats was very low. On the other hand, there was moderate muscle fiber degeneration (20.3-28%) in group II while in group III and IV the muscle fiber degeneration was severe (55.9-66%) and (82.7-90.2%) respectively.

The percent of caspase-3 positive fibers in the control group ranging from (0-1%). Higher percent was noticed in group II (8-10%). More caspase-3 immunopositive fibers were detected in groups III and IV. The percent was (40-60%) and (80-95%) for groups III and IV respectively.

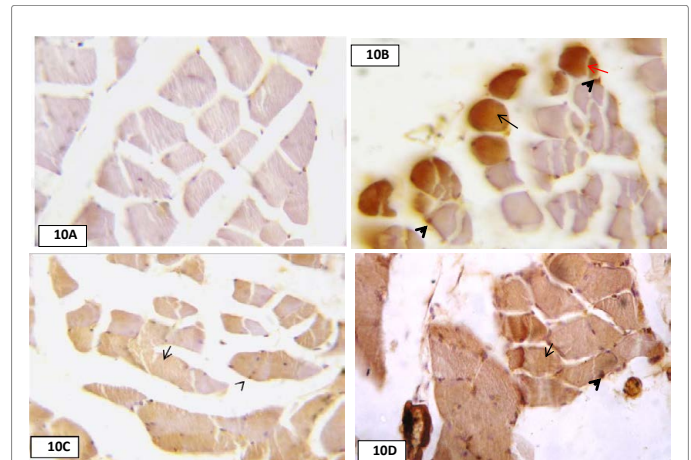


Figure 10: Caspase 3 immunohistochemical staining of skeletal muscle tissue of **A.** Control group showing negative immunoreactivity in the muscle fibers. **B.** Group II showing positive immunoreactivity in cytoplasm of some rounded muscle fibers (thin arrow). Notice some nuclei showing positive immunoreactivity (arrow heads) and many fibers showing splitting (red arrow). **C.** Group III showing positive immunoreactivity in cytoplasm of most of the muscle fibers (thin arrow). Notice nuclear expression (arrow head). **D.** Group IV showing positive cytoplasmic immune reaction in the muscle fibers (arrow). Some nuclei showing positive reaction (arrow heads). (immunohistochemistry counter stain H x 400).

Discussion

Prevention of major cardiovascular events (coronary events, coronary revascularization, and ischemic strokes) is one of the important roles of statins. Additional benefits with intensive statin therapy, and the prophylactic approaches against cardiovascular diseases, led to a widespread use of statins and the prescription of higher doses [5]. Although statins could be tolerated, many degrees of myopathy ranging from mild myalgia to rhabdomyolysis have been reported [1].

The present work was done to show the potential myotoxicity of atorvastatin and whether these effects are dose dependent or not. This study was also attempting to study the possible mechanisms beyond these changes using histological, histochemical and immunocytochemical techniques. Eng et al., [12] reported that vastus medialis of the quadriceps femoris muscle mostly are formed of type II white fibers. Statins affect type II muscle fibers mainly [11,13]. That is the reason for doing the current study on that muscle in particular. In the current study, different structural changes were detected in the skeletal muscle tissue of rats receiving 10, 40 or 80 mg/kg of atorvastatin.

Hematoxylin and eosin stain revealed focal areas with inflammatory cell infiltration, rounding and splitting of the muscle fibers. Fragmentation of the sarcoplasm and dense centrally located nuclei were also detected in all groups. These changes become more obvious with increasing the dose of atorvastatin. Marked damage of the muscle fibers noticed with the use of 80 mg/kg dose. This confirmed by grading of degeneration of muscle fibers. This was in agreement with Rallidis et al., [14] who reported that in clinical practice 5-10% of patients receiving statins develop myopathy, and this myopathy was dose dependent. Also this was in line with the study of Silva et al. [15] who reported a 10-fold increase in myopathy in patients taking a high dose of atorvastatin or simvastatin compared to patients on a lower dose. This study confirmed the finding of those studies through histological examination of the muscle fibers of treated rats with different doses of the drug.

Degeneration and inflammatory cellular infiltration in skeletal muscle fibers were noticed in this study. This was reported by many investigators using a variety of statins [16,7,17]. It could be suggested that the degenerative changes that affected the muscle fibers might be the stimulus that initiated the inflammatory reaction. This was explained by Stevnes and Lowe, [18], who stated that the degenerated fibers release different inflammatory mediators that lead to mononuclear cellular infiltration. Many markers were reported as signs of muscle fiber damage and degenerative myopathies as the central located nuclei observed in this study [19,20]. The splitting of the muscle fibers might be due to the insufficient oxygen supply and metabolites exchange to the enlarged and hypertrophied fibers [17].

In groups III and IV, some myofibers were noticed with linearly arranged euchromatic nuclei and often surrounded by many satellite cells. These findings might indicate the presence of regenerating fibers that usually appeared near areas of necrosis and degeneration [21]. After muscle injury, infiltrating inflammatory cells release cytokines and growth factors that might affect satellite cells leading to its activation and proliferation and finally to differentiation into myoblasts [22].

Using gleans stain, there were apparent degenerative changes affecting the nerve fibers. These changes may be in the form of thinning or disorganization of their neurofibrils leading to break up of the nerve fibers. The nerve fiber damage was extensive in rats receiving 80 mg/kg. The effects of statins on the nervous system are controversial, since some authors suggest neuroprotective effects whilst others have demonstrated that statins induced neuronal apoptosis [23]. A study conducted by Otruba et al., [24] confirmed definite damage to peripheral nerves in patients taking statins for more than 2 years. Inhibition of 3-hydroxy-3-methyl glutaryl coenzyme A (HMG-CoA) pathway deprives the cell from important antioxidant molecules such as ubiquinone or coenzyme Q10 [11]. This will cause production of free radicals, which affect the nerve cells [25]. In contrast, many studies reported that the serum coenzyme Q10 levels decrease during statin treatment but its myocyte levels are not consistently decreased [14].

Succinate dehydrogenase, a constitutive molecule of complex II of the mitochondrial electron transport chain, has been reported to play an important role at high respiration rates, and its activity has been considered a good indicator of the mitochondrial oxidative capacity [26]. The vastus medialis was consisting mostly of low oxidative (lightly stained) fast twitch fibers (type II) with few high oxidative (deeply stained) slow twitch fibers (type I). In this study, there was a decrease in succinate dehydrogenase (SDH) activity started in type II (lightly stained) fibers in low doses. With increasing the dose both type I and II were affected. The central and eccentric absence of oxidative enzyme reaction (SDH) in all muscle fibers was noticed in the central core disease myopathy. These regions represent areas of absence of mitochondria and distortion of myofilaments when examined ultrastructurally [27]. Hassan et al., [17] suggested an involvement of mitochondria with statin treatment. It was reported that statins inhibit the HMG-CoA-reductase which results in low intracellular cholesterol levels. Low intracellular cholesterol levels modulate fluidity of cell membranes. This in turn alters in the Na⁺/K⁺ pump function leads to degeneration of the membranous organelles of muscle fibers [28]. Sirvent et al., 2005 [29] reported that simvastatin induces an efflux of Ca²⁺ from the mitochondria of isolated human muscle fibers. This efflux is caused by a disruption in mitochondrial function. Altered Ca²⁺ homeostasis leads to muscle dysfunction and dysregulation.

AChE is an important component of all cholinergic synapses in the central and peripheral nervous systems. It rapidly hydrolyzes

acetylcholine released from the nerve terminals [30]. It is well established that AChE activity is also influenced by the pattern of nerve impulses, muscle electromechanical activity and neurogenic substances conveyed by axonal transport [31]. The levels of AChE mRNA decrease following skeletal muscle denervation [32].

In the present work, histochemical finding of the skeletal muscle tissue of the 10 mg/kg treated group showed that the acetylcholine esterase (AChE) staining did not affected. On the other hand, there was a reduction in AChE staining at dose of 40 mg/kg. At dose of 80 mg/kg, the intensity of staining decreased. In addition, there were small sized neuromuscular junction (NMJ) areas. The intensity of AChE staining reflects its activity as reported by Wen et al., [31]. While Liu et al., [33] suggested that the density of AChE staining reflects the amount of AChE in the NMJ and the size of the AChE-positive region reflected the size of the NMJ. This result was in agreement with Cibickova et al., [34] who found that low doses of atorvastatin (10 or 20 mg/kg) did not affect acetylcholine esterase activity. We could not report any study investigate the effect of high doses of statin on the AChE.

Vignaud et al., [35] showed that the AChE deficiency in mice results in reduced muscle weight and absolute maximal isometric force. Muscle weakness has also been reported in humans deficient in endplate AChE [36]. It has been well documented that a deficiency of AChE results in a change in hind limb muscle function and decreased ability of the hind limb to resist fatigue [37]. The decrease of the AChE activity observed would lead to an incomplete hydrolysis of the acetylcholine (ACh), and its accumulation at the synaptic cleft [31].

Using myosin heavy chain antibodies, two types of muscle fibers could be demonstrated, the more numerous immunopositive type II fast twitch fibers and the less numerous slow myofibers (type I) that remained unstained. In this study, it was found that in the vastus medialis of the quadriceps femoris muscle with a high content of type II fibers, there was quite degeneration of the type II fibers with essentially total sparing of the type I fibers in rats receiving 10 or 40 mg/kg. However, affection of the type I fibers was observed in 80 mg/kg treated group.

These histological findings were in a good agreement with Westwood et al., [11] who found that muscles showing the most severe necrosis following administration of statin contained a substantial proportion of type II fibers, and in these muscles it was the type II fibers that become degenerated first and the type I fibers were least sensitive to statins. The observation that statin myotoxicity affects type II, glycolytic muscle fibers more than type I, oxidative fibers [16] could be explained by decreased mitochondrial number/function in pale, glycolytic muscle enhances susceptibility to muscle damage and wasting. This observation could be also explained by the protective effect of PGC-1 α gene expression which is greater in oxidative fibers [13]. Overexpression of PGC-1 α gene, a transcriptional coactivator that induces mitochondrial biogenesis and protects against the development of muscle atrophy, dramatically prevented statin-induced muscle damage [38].

Caspases play a key role in apoptosis [39]. Immunohistochemical localization of activated (cleaved) caspase 3 in rat skeletal muscle tissues as an indicator of apoptosis was performed. In this study, the percent of caspase 3-immuno positive muscle fiber in the control rats was very low. In the other hand, the percent of the caspase 3-immuno positive muscle fibers increased with higher doses. This was in agreement with the study of Mazroa and Asker, [19] who observed the expression of active caspase 9 in rat skeletal muscle after 10 mg/kg of atorvastatin

treatment and the study of Urso et al., [40] who found that atorvastatin induces apoptosis in the skeletal muscle at a genetic level. Different statins can induce apoptosis in skeletal muscle [41]. This result was explained by Rallidis et al., [14] who reported that statin induced myotoxicity through the depletion of isoprenoids that control the rate of myofiber apoptosis. Isoprenoids are linked to proteins by either farnesylation or geranylgeranylation. The reduction of these proteins increases cytosolic calcium, which activates a cascade of events leading to the activation of caspase-3.

In spite of all the degenerative findings encountered in the present study and in other studies, some researches considered atorvastatin and the other statins safe to use even in high doses [42] and consider statins the most effective prescribed drugs for lowering serum cholesterol [43] not only by inhibiting cholesterol synthesis, but also through other mechanisms.

Conclusions

It can be concluded that atorvastatin has toxic effect on the skeletal muscle and its nerve supply and this effect is dose dependent. This toxic effect involves type II muscle fibers with low dose while type I fibers affected with high dose. Early involvement of the mitochondria, skeletal muscle fibers apoptosis and decreased AChE activity could be the mechanisms through which atorvastatin induces its toxic effect.

References

1. Soner BC, Inan SY, Guven U, Oktem G, Sahin AS (2013) Combined treatment with resveratrol prevents the atorvastatin-induced myopathy in rat skeletal muscle. *Afr J Pharm Pharmacol* 7: 1114-1118.
2. Sweetman Sean C (2009) Cardiovascular drugs. Martindale: the complete drug reference (36th edn.). London: Pharmaceutical Press pp: 1155-434.
3. Grundy SM, Cleeman JI, Merz CNB, Brewer HB, Clark LT, et al. (2004) Implications of recent clinical trials for the National Cholesterol Education Program. Adult Treatment Panel III guidelines. *Circulation* 110: 227-239.
4. Graveline D, Blair PW (2016) Statin Effects on Muscle and Kidney. *Journal of American Physicians and Surgeons* 21.
5. Parkin L, Paul C, Herbison GP (2014) Simvastatin dose and risk of rhabdomyolysis: Nested case-control study based on national health and drug dispensing data. *Int J Cardiol* 174: 83-89.
6. Vaughan CJ, Gotto AM (2004) Update on Statins: 2003. *Circulation* 110: 886-892.
7. Pierno S, Didonna MP, Cippone V, De Luca A, Pisoni M, et al. (2006) Effects of chronic treatment with statins and fenofibrate on rat skeletal muscle: a biochemical, histological and electrophysiological study. *Br J Pharmacol* 149: 909-919.
8. Schmechel A, Grimm M, El Armouche A, Höppner G, Schwoerer AP, et al. (2009) Treatment with atorvastatin partially protects the rat heart from harmful catecholamine effects. *Cardiovasc. Res.* 82: 100-106.
9. Bancroft J, Garbo M (2008) Theory and practice of histological techniques. 6th (edn.) Harcourt: Churchill Livingstone: 126, 127, 417, 422 and 425.
10. Krajewska M, Wang HG, Krajewski S, Zapata JM, Shabaik A (1997) Immunohistochemical analysis of *in vivo* patterns of expression of CPP32 (Caspase-3), a cell death protease. *Cancer Res.* 57: 1605-1613.
11. Westwood FR, Bigley A, Randall K, Marsden AM, Scott RC (2005) Statin-induced muscle necrosis in the rat: Distribution, development and fibre selectivity. *Toxicol Pathol* 33: 246-257
12. Eng CM, Smallwood LH, Rainiero MP, Lahey M, Ward SR, et al. (2008) Scaling of muscle architecture and fiber types in the rat hindlimb. *J Exp Biol* 211: 2336-2345.
13. Hanai J, Cao P, Tanksale P, Imamura S, Koshimizu E, et al. (2007) The muscle specific ubiquitin ligase atrogin-1/MAFbx mediates statin-induced muscle toxicity. *J Clin Invest* 117: 3940-3951.
14. Rallidis LS, Fountoulaki K, Anastasiou-Nana M (2011) Managing the underestimated risk of statin-associated myopathy. *Int J Cardiol.*
15. Silva M, Matthews ML, Jarvis C, Nolan NM, Belliveau P (2007) Meta-analysis of drug-induced adverse events associated with intensive-dose statin therapy. *Clin Ther* 29: 253-60.
16. Schaefer WH, Lawrence JW, Loughlin AF, Stoffregen DA, Mixson Dean (2004) Evaluation of ubiquinone concentration and mitochondrial function relative to cerivastatin-induced skeletal myopathy in rats. *Toxicol. Appl Pharmacol* 1: 10-23.
17. Hassan NF, El-Bakry NA, Shalaby NM, Ghobara MM, Bayomi NA (2009) Histological Study of the Effect of Simvastatin on the Skeletal Muscle Fibers in Albino Rat and the Possible Protective Effect of Coenzyme Q 10. *Egypt. J Histol* 31: 216-226.
18. Stevnes A, Lowe J (2000) Tissue response to damage. In: Stevnes A, Lowe J, edtr. *Pathology.* (2nd ed.) Mosby pp: 35-60.
19. Mazroa, SA, Asker SA (2010) Myotoxic Effects of Atorvastatin Drug (Lipitor) on the Skeletal Muscles of Adult Male Albino Rats and the Effect of L-Carnitine Co-administration Light Microscopical, Immunohistochemical and Biochemical Study. *Egypt. J Histol* 33: 520- 531
20. Sugarman MC, Yamasaki TR, Oddo S, Echegoyen JC, Murphy MP (2002) Inclusion body myositis-like phenotype induced by transgenic overexpression of beta APP in skeletal muscle. *U.S.A. 30: Proc Natl Acad Sci* 6334-6339.
21. Mann CJ, Perdiguero E, Kharraz Y, Aguilar S, Pessina P (2011) Aberrant repair and fibrosis development in skeletal muscle. *Skelet Muscle* 4: 21
22. Tidball JG, Villalta SA (2010) Regulatory interactions between muscle and the immune system during muscle regeneration. *Am J Physiol Regul Integr Comp Physiol* 298: R1173-1187.
23. Park DS, So HS, Lee JH, Park HY, Lee YJ (2009) Simvastatin treatment induces morphology alterations and apoptosis in murine cochlear neuronal cells. *Acta Otolaryngol* 129: 166-74.
24. Otruba P, Kanovsky P, Hlustik P (2011) Treatment with statins and peripheral neuropathy: results of 36-months a prospective clinical and neurophysiological follow-up. *Neuro Endocrinol Lett* 32: 688e90.
25. Kempler P, Varkonyi T (2012) *Neuropathies-A global Clinical Guide.* Budapest: Zafir Press
26. Fattoretti P, Vecchiet J, Felzani G, Gracciotti N, Solazzi M (2001) Succinic dehydrogenase activity in human muscle mitochondria during aging: a quantitative cytochemical investigation. *Mechanisms of Ageing and Development* 122: 184-1848.
27. Thaha F, Gayathri N, Nalini A (2011) Congenital myopathies: Clinical and immunohistochemical study. *Neurology India* 59: 879-883.
28. Carvalho AA, Lima UW, Valiente RA (2004) Statin and fibrate associated myopathy: Study of eight patients. *Arq. Neuropsiquiatr* 62: 257-261.
29. Sirvent P, Mercier J, Vassort G, Lacampagne A (2005) Simvastatin triggers mitochondria-induced Ca²⁺ signalling alteration in skeletal muscle. *Biochem Biophys Res Commun* 329: 1067-75.
30. Van der Kloot W, Molgo J (1994) Quantal acetylcholine release at the vertebrate neuromuscular junction. *Physiol Rev* 74: 899-991.
31. Wen G, Hui W, Dan C, Xiao-Qiong W, Jian-Bin T (2009) The Effects of Exercise-induced Fatigue on Acetylcholinesterase Expression and Activity at Rat Neuromuscular Junctions. *Acta Histochem Cytochem* 42: 137-142.
32. Michel RN, Vu CQ, Tetzlaff W, Jasmin BJ (1994) Neural regulation of acetyl cholinesterase mRNAs at mammalian neuromuscular synapses. *J Cell Biol* 127:1061-1069.
33. Liu R, Xu H, Wang G, Li J, Gou L (2013) Extraocular Muscle Characteristics Related to Myasthenia Gravis Susceptibility. *PLoS ONE* 8: e55611.
34. Cibickova L, Hyspler R, Micuda S, Cibicek N, Zivna H (2008) The influence of simvastatin, atorvastatin and high-cholesterol diet on acetyl cholinesterase activity, amyloid beta and cholesterol synthesis in rat brain. *Steroids* 74: 13-9.
35. Vignaud A, Fougereuse F, Mouisel E, Guerchet N, Hourde Bacou F (2008) Genetic inactivation of acetyl cholinesterase causes functional and structural impairment of mouse soleus muscles. *Cell Tissue Res* 333: 289-296.

36. Ohno K, Engel AG, Brengman JM, Shen XM, Heiden-Reich F (2000) The spectrum of mutations causing end-plate acetyl cholinesterase deficiency. *Ann Neurol* 47: 162-170
37. Chau DT, Rada P, Kosloff RA (2001) Nucleus accumbens muscarinic receptors in the control of behavioral depression: antidepressant-like effects of local M1 antagonist in the Porsolt swim test. *Neuroscience* 3: 791-798.
38. Mootha VK, Handschin C, Arlow D, Xie X, St Pierre J (2004) Erralpha and Gabpa/b specify PGC-1alpha-dependent oxidative phosphorylation gene expression that is altered in diabetic muscle. *USA Proc Natl Acad Sci* 101: 6570-6575.
39. Shi Y (2004) Caspase activation: revisiting the induced proximity model. *Cell* 117: 855-858.
40. Urso ML, Clarkson PM, Hittel D, Hoffman EP, Thompson PD (2005) Changes in ubiquitin proteasome pathway gene expression in skeletal muscle with exercise and statins. *Arterioscler Thromb Vasc Biol* 25: 2560-2566.
41. Yu JG, Sewright K, Hubal MJ, Liu JX, Schwartz LM (2009) Investigation of gene expression in C2C12 myotubes following simvastatin application and mechanical strain. *J Atheroscler Thromb* 16: 21-29.
42. Ara R, Pandor A, Stevens J, Rees A, Rafia R (2009) Early high-dose lipid-lowering therapy to avoid cardiac events: A systematic review and economic evaluation. *Health Technol. Assess* 13: 3-94.
43. Mohaupt MG, Karas RH, Babychuk EB, Sanchez Freire V, Monastyrskaya K (2009) Association between statin-associated myopathy and skeletal muscle damage. *CMAJ* 181: E11-E18.